JRMP Journal of Radiopharmaceuticals and Molecular Probes Vol. 7, No. 2, Dec. 2021
J Radiopharm Mol Probes 2021;7(2):79-84
ISSN 2384-1583(Print) / ISSN 2508-3848(Online)

Original Articles

https://doi.org/10.22643/JRMP.2021.7.2.79

Synthesis of a PEGylated tracer for radioiodination and evaluation of potential in tumor targeting

Abhinav Bhise, Sushil K Dwivedi, Kiwoong Lee, Jeong Eun Lim, Subramani Rajkumar, Woonghee Lee, Seong Hwan Cho, Jeongsoo Yoo*

Department of Molecular Medicine, Brain Korea 21 Four KNU Convergence Educational Program of Biomedical Sciences for Creative Future Talents, School of Medicine, Kyungpook National University, Daegu 41944, Korea.

ABSTRACT

Radiopharmaceuticals are important for tumor diagnosis and therapy. To deliver a radiotracer at the desired target excluding non-targeted tissues is difficult. The development of a targeted tracer that has a good clearance profile while maintaining high biostability and biocompatibility is key to optimizing its biodistribution and transport across biological barriers. Improving the hydrophilicity of radiotracers by PEGylation can reduce serum binding, allowing the tracer to circulate without retention and reducing its affinity for non-targeted tissues. In this study, we synthesized a new benzamido tracer (SnBz-PEG_{36}) with the introduction of a low molecular weight polyethylene glycol unit (PEG_{36}, ~2,100 Da). The tumor targeting efficiency and biodistribution of [^{131}I]-Bz-PEG_{36} or radiotracer-loaded liposomes were evaluated after their administration to normal mice or mouse tumor models including CT26 (xenograft) and 4T1 (xenograft and orthotopic). Most of the radiotracer was cleared out rapidly (1-24 h post-administration) through the kidney and there was little tumor uptake.

Key Word: Radioiodination, PEG, Rapid clearance, Biodistribution, Tumor targeting

Introduction

The selective tumor targeting of a radiotracer while excluding accumulation in normal tissues is difficult. A long-standing dilemma in the field of diagnostics or therapeutics is the reticuloendothelial system uptake of molecules. Indeed, the physicochemical properties of radiotracers including their hydrodynamic size, molecular weight, overall chargedistribution, hydrophilicity, and hydrophobicity have a role in preventing their uptake in non-targeted tissues (1). After their administration in vivo, most molecules are eliminated through the kidneys via renal tubular secretion or glomerular filtration (2). In general, molecules with a molecular weight < 40 kDa are transported through the glomerular filtration membrane (3, 4). However, renal clearable molecules were also reported to be eliminated via the influx-efflux mechanism into the proximal tubules (5). The main role of radiotracers is to target cancers with rapid clearance and provide enhanced signals in any modality imaging (6). Considering this, Bujie Du et al. reported the ICG-PEG45 molecule, which selectively targets renal cell carcinomas via renal tubular secretion

Received: November 16, 2021 / **Revised:** December 27, 2021 / **Accepted:** December 28, 2021

Correspnding Author : Jeongsoo Yoo, Department of Molecular Medicine, School of Medicine, Kyungpook National University,680 Gukchaebosang-ro, Joong-gu, Daegu 41944, Korea.
Tel: +82-53-420-4947, Fax: +82-53-426-4944, E-mail: yooj@knu.ac.kr

(7). Due to its low affinity towards the mononuclear phagocytic system (MPS), which includes the liver and spleen, molecules that interact with organic anion transporters in the proximal tubules undergo influx on the basolateral side and efflux via the P-glycoprotein (P-gP) transporter. Notably, ICG-PEG45 was not only limited to kidney carcinomas but also detected metastatic tumors with positive contrast in other organs such as the brain, bone, and lungs.

Liposomes are non-toxic, biodegradable, and biocompatible materials that are ideal drug carriers because they are morphologically identical to the host cell structure and can encapsulate various substances (8, 9). Several biomedical applications ofvarious liposomes have been already approved by the Food and Drug Administration and many are in clinical trials (10). However, to be effective, lipo- somes should be loaded with any diagnostic or therapeutic agent and many optical or nuclear tracers are well established (11). Based on these previous studies, we designed and synthesized a new tracer, SnBz-PEG_{36}, which contains low molecular weight polyethylene glycol (PEG_{36}) that improves hydrophilicity and reduces affinity towards the MPS, and which can undergo radioiodination for use as a nuclear diagnostic tool. Because of the advantages of liposomes in delivering such agents, we prepared liposomes and evaluated them in tumor models in comparison with a radiotracer. The radiotracer and liposomes were rapidly cleared in normal mice or mouse tumor models, with low tumor uptake.

Materials and Methods

General remarks

Amino-PEG_{36} carboxylic acid was purchased from Broad- Pharm (San Diego, CA, USA), and all remaining reagentswere purchased from Sigma-Aldrich (St. Louis, MO, USA)unless otherwise noted. [^{131}I]NaI was provided by SamyoungUnitech (Daejeon, Korea) and 1,2-dipalmitoyl-sn-glycero-3-phosphocholine (DPPC), cholesterol, and 1,2-distearoylsn-glycero-3-phosphoethanolamine-N-[methoxy(polyethyleneglycol)-2000] (DSPE-PEG2000), were purchased from Avanti Polar Lipids (Alabaster, AL, USA). Phosphate-buffered saline (PBS) was purchased from HyClone (Logan, Utah,USA). The tracer was purified via HPLC (Waters Corp.,Milford, MA, USA) using a Luna C8 HPLC column(Phenomenex, Torrance, CA, USA).

Synthesis of 2, 5-dioxopyrrolidin-1-yl 4-iodobenzoate (2)

4-iodobenzoic acid (500.0 mg, 2.01 mmol) was added to a stirred solution of 1-hydroxypyrrolidine-2,5-dione (255.15 mg, 2.21 mmol) and 1-ethyl-3-(3-dimethylaminopropyl)carbodiimide (343.08 mg, 2.21 mmol) in CH_2Cl_2 (10 mL). The reaction mixture was stirred at room temperature for 8 h. After completion of the reaction (monitored by TLC), the solvent was evaporated under reduced pressure. Ice cold water was added to the crude form and then extracted with CH_2Cl_2 (3 × 10 mL). The combined organic phase was washed in brine and dried over $MgSO_4$. The solvent was concentrated to give an off-white solid. After purification by column chromatography on a silica mesh, elution with hexane/ethyl acetate (7:3) obtained 2,5-dioxopyrrolidin-1-yl 4-iodobenzoate as a white solid (496.71 mg, 72% yield). ^{1}H NMR (500 MHz, $CDCl_3$): δ 2.93 (s, 4H), 7.84 (d, J = 9 Hz, 2H), 7.90 (d, J = 8.5 Hz, 1H) ppm.

Synthesis of 2, 5-dioxopyrrolidin-1-yl 4-(tributylstannyl) benzoate (3)

Hexabutylditin (0.78 ml, 0.9 g, 1.55 mmol) and a catalytic amount of tetrakis(triphenylphosphine)palladium (3.0 mol %) were added to a stirred solution of 2.5-

dioxopyrrolidin-1-yl 4-iodobenzoate (240.49 mg, 0.97 mmol) in anhydrous toluene (10.0 ml). The reaction mixture was refluxed for 8 h. After completion of the reaction (monitored by TLC) the reaction mixture was cooled at an ambient temperature and the reaction mixture was filtered. The filtrate was evaporated under reduced pressure to obtain a black thick oil. After purification by column chromatography on a silica mesh, elution with hexane/ethyl acetate (7:3) obtained 2,5-dioxopyrrolidin-1-yl 4-(tributylstannyl)benzoate as a colorless oil (201.0 mg, 40% yield). ^{1}H NMR (500 MHz, $CDCl_3$): δ 0.96-0.89 (m, 9H), 1.14-1.10 (m, 4H), 1.37-1.32 (m, 8H), 1.57-1.52 (m, 6H), 2.92 (s, 4H), 7.65 (d, J = 8.0 Hz, 2H), 8.06 (d, J = 8.0 Hz, 2H) ppm.

Synthesis of SnBz-PEG$_{36}$ (4)

2,5-dioxopyrrolidin-1-yl 4-(tributylstannyl)benzoate (3.0 mg, 5.9 μmol) and amino-PEG$_{36}$ carboxylic acid (10.0 mg, 6.0 μmol) were added to 3.0 mL CH_2Cl_2 followed by the addition of triethylamine (~2.0 μL, 20.0 μmol). The reaction mixture was stirred at room temperature for 16 h. After completion of the reaction (monitored by TLC), the solvent was evaporated under reduced pressure. Ice cold water was added to the crude form and extracted with CH_2Cl_2 (3 × 5 mL). The combined organic phases were washed with cold water and dried over $MgSO_4$. The solvent was concentrated to give an off-white solid. Further purification was carried out using semi-preparative HPLC (WATERS) with a Phenomenex Luna C8 column (5 μm x 10 x 50 mm) by eluting a gradient containing 0.1% TFA/H_2O (A) and 0.1% TFA/ACN (B); 0-20% (B) for 5 mins and 20-90% (B) for 30 mins, followed by 90-0% (B) for 40 mins with a flow rate of 1 mL/min at 254 nm. Finally, collected fractions were frozen at -80 ℃ and lyophilized to obtain 2,5-dioxopyrrolidin-1-yl 4-iodobenzoate (SnBz-PEG$_{36}$) as a white solid (3.3 mg, ~ 30% yield). Matrix-assisted laser desorption ionization-time of flight (MALDI-TOF) m/z: calculated $[M+Na]^+$: 2091.1409; found: 2091.0881.

Radioiodination of SnBz-PEG36 (5)

1 M HCl and [^{131}I]NaI (11.1 MBq) were added to an aliquot of 100 μg/100 μL of radiotracer in acetic acid, and vortexed. Radioiodination was initiated by adding 3% hydrogen peroxide and thermomixed for 30 mins at 70°C. The reaction was monitored by radio-TLC (silica, hexane/ethyl acetate; 20:1) and after the completion of iodination, it was quenched by $NaHSO_3$. The reaction mixture was evaporated to dryness at 50 °C for 30 mins to evaporate the free radioiodine. Purified [^{131}I]-Bz-PEG$_{36}$ was dissolved in chloroform and used for tumor targeting study or liposome preparation.

Liposome preparation of [^{131}I]-Bz-PEG$_{36}$

The radiotracer-loaded liposomes were prepared as previously reported (12). Briefly, [^{131}I]-Bz-PEG$_{36}$ was added to a mixture of liposomal components, 0.5 mM of DPPC, DSPE-PEG2000, and cholesterol in $CHCl_3$ at a molar ratio of 16:7:1 in a 100-mL round bottom flask. The lipids were evaporated for 30 mins on a rotary evaporator at slow rotation to obtain a thin film. Next, the thin lipid film was hydrated using 1 mL PBS at a transition temperature of 55 °C for 30 mins. The radio-liposomal dispersion was extruded by passing through 400 nm and 100 nm polycarbonate membranes (Whatman, Kent, UK) 21 times from each membrane using a mini extruder (Avanti, Polar Lipids, USA).

Animal models

To evaluate the targeting ability and clearance of [^{131}I]-Bz-PEG$_{36}$ in mouse tumor models, CT26 cells and 4T1/Luc$^+$ cells were subcutaneously inoculated into the right (1 × 10^6 cells per mouse) and left shoulder (5 × 10^6 cells per mouse) of BALB/c mice (male, 7 weeks, 16 - 20 g,

Hyochang Science, Daegu, Korea). When the tumor reached 6-8 mm in diameter (8 days after inoculation), biodistribution studies with [^{131}I]-Bz-PEG$_{36}$ were conducted in xenograft models. Orthotopic pancreatic tumor models were prepared by the inoculation of 4T1/Luc^{+} cells (1×10^{6} cells per mouse) into the pancreatic tail of C57BL/6J mice (male, 7 weeks 16-20 g, Hyochang Science, Daegu, Korea).

Biodistribution studies

Biodistribution studies were conducted using [^{131}I]-Bz-PEG$_{36}$ (0.5-0.8 MBq in 200 μL PBS) in normal mice or mouse tumor models (n = 1 each). All samples were intravenously injected through the tail vein and mice were anesthetized using 1-2% isoflurane in O_2. Post-injection mice were sacrificed and organs were harvested at 24, 23, 4, and 1 h time points in normal mice, 4T1 (orthotopic), CT26, and 4T1 (xenograft) mouse models, respectively. Harvested organs were weighed immediately and measured by γ-Counter (Wallach, Turku, Finland). The biodistribution data were shown as a percentage of the injected dose per weight (%ID/g).

Results and Discussion

Preparation of the SnBz-PEG$_{36}$ tracer (4)

The three-step synthesis was initiated from commercially available 4-iodobenzoic acid to yield 4-iodobenzoate-NHS ester with the help of a carboxyl activating agent, EDC. Here, we selected 4-iodobenzoic acid as the core due to its high stability and to minimize *in vivo* deiodination. Further stannylation of aryl halide was performed under refluxing conditions in the presence of a catalytic amount of Pd(PPh$_3$)$_4$. Finally, amino-polyethylene glycol (PEG$_{36}$) was coupled with stannylated benzoate in the presence of a strong base, triethylamine, to yield the tracer, SnBz-PEG$_{36}$ (4) (Scheme 1). The tracer was then purified by preparative high-pressure liquid chromatography with the help of a reverse phased C8 column (RP-HPLC) with an overall yield of 8.64% and MALDI-TOF analysis confirmed the formation of the tracer (Figure 1).

Radioiodination of SnBz-PEG$_{36}$ (5)

Radioiodination was performed by replacing the tributylstannyl group of (4) with radioactive iodine-131 (Figure 2). Simply, in the presence of acetic acid and hydrogen peroxide, the tracer and [^{131}I]NaI (11.1 MBq) were agitated together at 70°C for 30 mins. The iodination was monitored by thin-layer chromatography spotting the mixture on iTLC-SG and was developed in 50 mM ammonium citrate. The free iodine moves towards the front line whereas the tracer remains at the origin because of its bulkier nature. After confirmation of radioiodination, the reaction was quenched by sodium bisulfite, and the mixture was extracted using acetonitrile on a rotary evaporator and reconstituted in PBS and in chloroform for liposome preparation to examine individual and liposome-loaded tumor targeting.

Preparation of liposome-loaded tracers

For the encapsulation of a radiotracer into liposomes, we followed our optimized and reported protocol (12). All the lipids, DPPC, cholesterol, and DSPE-PEG2000 were dissolved in chloroform to a final concentration of 0.5 mM and mixed together with [^{131}I]-Bz-PEG$_{36}$ at a molar ratio of 16:1:7. The mixture was concentrated over a rotary evaporator to form a thin lipid film, which was then hydrated in PBS at 55°C for 30 mins. The tracer-loaded liposomal solution was extruded through 400 nm and 100 nm membrane filters using a manual extruder. Finally, the uniformed liposomes were admin-

istered to the mouse tumor models and further biodistribution studies were performed.

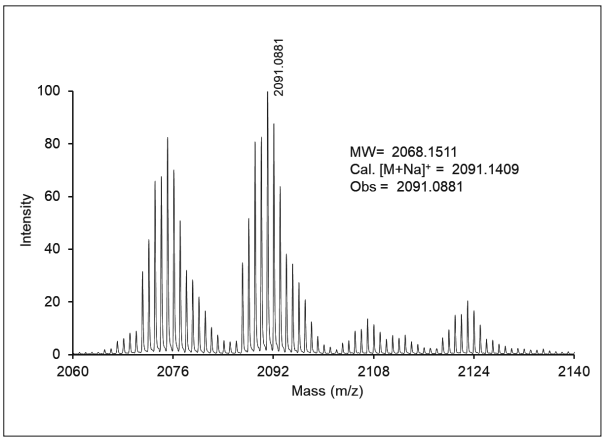

Figure 1. Characteristic MALDI-TOF spectrum of SnBz-PEG$_{36}$ (4).

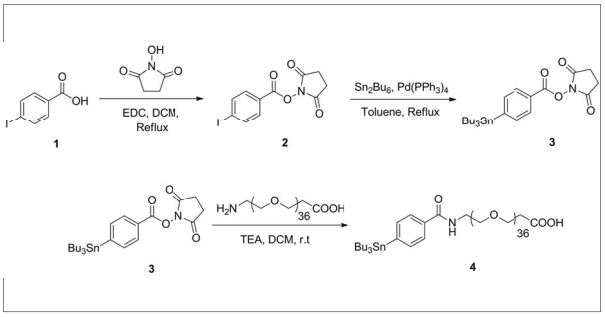

Scheme 1. Synthetic route of the intermediate 4-stannyl-NHS ester (3) and radiotracer SnBz-PEG$_{36}$ (4).

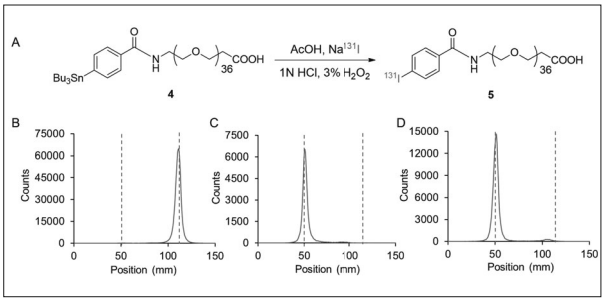

Figure 2. Radiolabeling of SnBz-PEG$_{36}$ (A), radio-TLC profile of free [^{131}I]NaI (B), radio-iodinated [^{131}I]-Bz-PEG$_{36}$ (C), and radio-TLC final extruded liposomes (D). All TLCs were developed in 50 mM ammonium citrate as the mobile phase and iTLC-SG as the stationary phase.

Evaluation of [^{131}I]-Bz- PEG$_{36}$ and loaded liposomes in mice

First, we investigated the affinity of the radiotracer [^{131}I]-Bz-PEG$_{36}$ to MPS in normal BALB/c mice. The radiotracer [^{131}I]-Bz-PEG$_{36}$ (0.7 MBq) was administered to mice through the tail vein and biodistribution studies were performed at 24 h post-injection. The tracer showed no affinity towards the liver or spleen and the maximum level was found in the kidneys (0.22% ID/g). In accordance with the study by Bujie Du et al. that showed ICG-PEG45 targeted metastatic tumors, we investigated the radiotracer in a 4T1 orthotopic carcinoma model. At 23 h post-injection, similar results were obtained as in normal mice: approximately 0.18% ID/g was present in the kidneys and only 0.01% was present in the 4T1 pancreatic tumor. Next, we screened the radiotracer in another tumor model (CT26 colorectal cancer). Due to its rapid clearance, mice were sacrificed at an earlier time point at 4 h post-injection. Slightly different results were observed in CT26 tumor mice. The thyroid (0.23% ID/g) and bone (0.12% ID/g) showed some uptake along with minimum tumor uptake (0.2% ID/g); however, there was less accumulation in the kidneys (0.06% ID/g) (Figure 3).

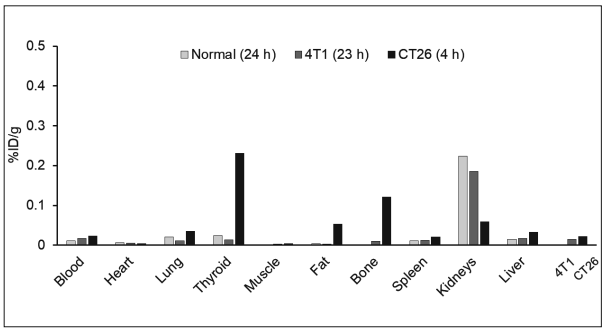

Figure 3. Biodistribution studies of radio-iodinated [^{131}I]-Bz-PEG$_{36}$ at 24, 23, and 4 h post-injection in normal mice (n=1), 4T1 (n=1) orthotopic and, CT26 (n = 1) xenograft tumor models, respectively.

These initial findings suggested that the radiotracer was cleared rapidly and had no strong affinity towards tumors. Finally, we decided to encapsulate [^{131}I]-Bz-PEG$_{36}$ into liposomes and monitored its delivery to the tumor site. The one-pot liposomes loaded with tracer were prepared and administered to the 4T1 xenograft mouse model by intravenous injection. Radiotracer-loaded liposomes showed little tumor uptake (0.36% ID/g) at

1 h post-injection, whereas the kidney and liver had the highest uptake (0.97% ID/g and 0.72 % ID/g, respectively; Figure 4). Overall, rapid clearance was observed for the radiotracer and liposomes, which had a poor affinity towards the MPS or tumor site, as confirmed at various timepoints and in different tumor models.

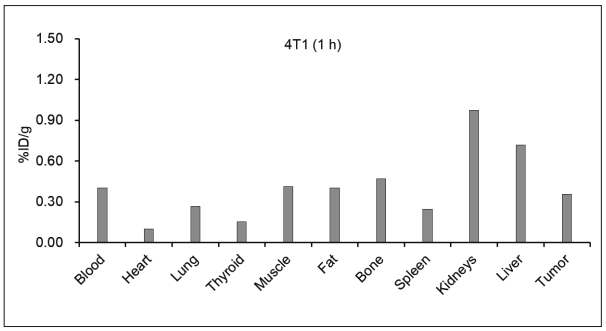

Figure 4. Biodistribution studies of radiotracer-loaded [^{131}I]-Bz-PEG$_{36}$-liposomes at 1 h post-injection in 4T1 xenograft mice (n = 1).

Conclusion

A new radiotracer with low molecular weight polyethylene glycol (SnBz-PEG$_{36}$) was synthesized and radioiodinated with iodine-131 to investigate its characteristics *in vivo*. As anticipated, the radiotracer was excreted through the kidneys with minimum or no affinity for the liver according to biodistribution studies. Similarly, we expected the radiotracer alone to target tumors; however, the tracer was cleared rapidly without targeting the tumors. We then loaded the radiotracer into liposomes and its tumor targeting ability was investigated; however, only 0.3% ID/g of the liposomes accumulated at the tumor site. Therefore, the radiotracer should be optimized further using higher numbers of mice.

Acknowledgment

This work was supported by an R&D program through the National Research Foundation of Korea funded by the Ministry of Science, ICT & Future Planning (Nos.2019 H1D3A1A01102643 and 2020R1C1C1008442).

References

1. Rosenblum D, Joshi N, Tao W, M. Karp J, Peer D. Progress and challenges towards targeted delivery of cancer therapeutics. ***Nature communications*** 2018;9:1410.
2. Hall JE, Guyton and Hall Textbook of Medical Physiolog. TWELFTH ed. Elsevier Health Sciences; 2010. p. 310-313.
3. Haraldsson B, Nystrçm J, Deen WM. Properties of the Glomerular Barrier and Mechanisms of Proteinuria. ***Physiol Rev*** 2008;88,451-487.
4. Du B, Yu M, Zheng J. Transport and interactions of nanoparticles in the kidneys. ***Nat Rev Mater*** 2018;3:358-374.
5. Wang K, Kestenbaum B. Proximal Tubular Secretory Clearance A Neglected Partner of Kidney Function. ***Clin J Am Soc Nephrol*** 2018;13:1291-1296.
6. Bradbury MS, Phillips E, Montero PH, Cheal SM, Stambuk H, Durack JC, Sofocleous CT, Meester RJ, Wiesner U, Patel S. Clinically-translated silica nanoparticles as dual-modality cancer-targeted probes for image-guided surgery and interventions. ***Integr Biol*** 2013;5:74-86.
7. Du B, Chong Y, Jiang X, Yu M, Lo U, Dang A, Chen Y, Li S, Hernandez E, Lin JC, Hsieh J, Zheng J. Hyperfluorescence Imaging of Kidney Cancer Enabled by Renal Secretion Pathway Dependent Efflux Transport. ***Angew Chem Int Ed*** 2021;60:351-359
8. Pattni BS, Chupin VV, Torchilin VP. New Developments in Liposomal Drug Delivery. ***Chem Rev*** 2015;115:10938-10966.
9. Kluza E, Jacobs I, Hectors SJCG, Mayo KH, Griffioen AW, Strijkers GJ, Nicolay K. Dual-targeting of αvβ3 and galectin-1 improves the specificity of paramagnetic/fluorescent liposomes to tumor endothelium in vivo. ***J Controlled Release*** 2012;158:207-214.
10. Torchilin VP. Recent advances with liposomes as pharmaceutical carriers. ***Nat Rev Drug Discovery*** 2005;4:145-160.
11. Louie A. Multimodality Imaging Probes: Design and Challenges. ***Chem Rev*** 2010;110:3146-3195.
12. Lee W, An GI, Park H, Sarkar S, Ha YS, Huynh PT, Bhise A, Bhatt N, Ahn H, Pandya DN, Kim JY, Kim S, Jun E, Kim SC, Lee KC, Yoo J. Imaging Strategy that Achieves Ultrahigh Contrast by Utilizing Differential Esterase Activity in Organs: Application in Early Detection of Pancreatic Cancer. ***ACS Nano*** 2021;15:17348-17360.